

EBSD characterization of repetitive grain refinement in AZ31 magnesium alloy

S. M. Fatemi-Varzaneh^a, A. Zarei-Hanzaki^{a,1}, J. M. Cabrera^{b, c}, P.R. Calvillo^{b, c}

^a Department of Metallurgical & Materials Engineering, University of Tehran, Tehran, Iran

^b Departamento de Ciencia de Materialese Ingeniería Metalúrgica, ETSEIB, Polytecnic University of Catalonia, Av.Diagonal 647, 08028 Barcelona, Spain

^cFundación CTM , Plaza de la Ciencai 2, 08243, Manresa, Spain

Abstract

A polycrystalline Mg-3Al-1Zn was subjected to high plastic strains by applying accumulative back extrusion (ABE) process. Electron back scatter diffraction analyses were used to explore the grain refinement mechanisms. A novel grain refinement trend was found at large strains, where new recrystallized grains were repetitively refined through dynamic recrystallization. The grain size was diminishing continuously up to the fourth ABE pass, after which no further grain refinement was noticed upon successive passes.

Keywords: recrystallization; microstructure; deformation; electron diffraction

1. introduction

Magnesium alloys are expected to be one of the most promising structural materials for application in aerospace and automotive industries due to their low density and high specific strength [1, 2]. However, magnesium alloys exhibit poor formability and limited ductility at room temperature owing to their hexagonal close-packed (HCP) crystal structure. In order to exploit the benefits of magnesium alloys, there is considerable current interest in processing magnesium samples through the procedures involving the application of severe plastic deformation (SPD) [1, 3, 4]. In practice, these procedures are attractive because they lead to a very significant grain refinement down to submicrometer or even nanometer level. Thus, the grain refinement achieved by severe deformation may assist in counteracting the limited strength and ductility of magnesium at low temperatures [1, 5].

Corresponding author: A. Zarei-Hanzaki (zareih@ut.ac.ir)
[Tel:0098-21-61114116](tel:0098-21-61114116), Fax:0098-21-88006076

The microstructure and mechanical properties of magnesium produced by SPD methods has been the focus of several studies. However, the microstructural evolution and the mechanism of dynamic recrystallization (DRX) during SPD processing have received limited attention in the literature. Figueiredo and Langdon [6] proposed a model for the grain refinement of magnesium alloys during processing by equal channel angular pressing (ECAP). This model is based on the principles of dynamic recrystallization in which necklace-like distributions of fine grains are nucleated along conventional grain boundaries (GBs) and also along twin boundaries. A systematic study was also made by Su et. al. [7], where a mechanism based on the observations from microstructure evolution during ECAP was presented. In contrast to Figueiredo and Langdon's model [6], Su's results showed that continuous recovery, recrystallization and grain growth in shear bands play a key role in effective grain refinement during ECAP of AZ31 alloy. Summarizing the published results [6-8], it is realized that the nature of grain refinement mechanism in magnesium alloys is dependent upon the initial grain structure prior to deformation and the parameters involved in the SPD processing. As a result of the various possible structural and processing permutations, it follows that the diverse microstructural features can be reported for these materials after processing by SPD techniques [6-9], including different final grain sizes and various multi-modal grain size distributions. The detail understanding of the grain refinement mechanisms may provide a potential platform for direct tailoring the grain size distribution thereby improving the ductility.

Recently, an accumulative back extrusion (ABE) process was invented by two of the present authors and studied as a new continuous SPD process suitable for mass production [10, 11]. It has been also shown that ABE is effective in reducing the grain size of AZ31 magnesium alloy down to submicrometer ranges [6, 11, 12]. In the present study, ABE process has been employed to investigate the grain refinement mechanisms and special attention has been paid to the evolution of fine grains at latter passes. To fulfill this purpose, the microstructures of AZ31 alloy after successive ABE passes were examined using electron back scattered diffraction (EBSD) technique and field emission scanning electron microscopy (FE-SEM).

2. Experimental procedure

The experimental AZ31 alloy was received as a rolled plate (22 mm in thickness with a nominal composition of Mg-2.9%Al-0.85%Zn-0.7%Mn, wt.%). The initial average grain size

was 25 μm (not shown here). The cylindrical work-pieces for ABE processing were machined with the dimensions of $\text{H}8 \times \Phi 18 \text{ mm}^3$, the deformation axis of which was selected to be parallel to the initial rolling direction. Earlier reports have provided the detailed experimental information on the processing of the AZ31 alloy by ABE [10, 11]. The principle of the ABE technique is illustrated in Fig. 1. Each ABE pass includes two steps and imposes an equivalent strain of about 4 [12]. Briefly speaking, the first step of ABE consists of the back extrusion of the work-piece into the gap between the inner punch and the die. In the second step the back-extruded material is forged back to the initial cross section by the outer punch and this completes one ABE pass. The ABE process was conducted up to six passes at a ram speed of 10 mm/min and a temperature of 330°C. Samples were quenched in water right after processing within less than 1 second using an ejection system designed under the bottom of the die. To study the microstructural features during deformation, additional work-pieces were subjected to ABE but were removed and quenched immediately at intermediate stages of the process. The as-processed work-pieces were then sectioned along the extrusion direction and mechanically ground with SiC papers of grit sizes down to 4000. The polishing was done by colloidal silica slurry containing particles of 0.05 μm . For FE-SEM analysis the specimens were etched with a solution composed of 4 gr picric acid, 10 ml water, 10 ml acetic acid and 70 ml ethanol for about 3 seconds.

The microstructures were studied on the longitudinal section (ED–TD plane) for different deformation conditions using scanning electron microscope (FEG-SEM, Zeiss Ultra Plus) equipped with EBSD. The microstructural maps were derived from EBSD, which shows grains and sub-grains based on misorientation angle on adjacent points. To analysis microstructure, three scans were made over the cross section. At least 100 and 500 grains were considered for grain size measurement before and after ABE processing, respectively.

3. Results and discussion

The microstructure of the experimental alloy processed through the first ABE pass is shown in Fig. 2. After applying one ABE pass at 330°C, the recrystallized grains with mean grain size of 7 μm have covered about 82% of the obtained microstructure (Fig. 2). The analysis of the microstructure indicates that the new grains have been formed preferentially at the prior

1
2
3
4 grain boundaries (GBs). The details of microstructural evolution during ABE processing were
5 precisely given elsewhere [12].
6

7
8 Two types of DRX are commonly discussed in the literature, i.e. discontinuous DRX
9 (DDRX) and continuous one (CDRX) [8, 13, 15]. The DDRX, which is known as conventional
10 DRX, proceeds by nucleation and growth and is found primarily in many materials with low to
11 medium stacking fault energy (SFE) including magnesium alloys. Although, the occurrence of
12 DRX in magnesium has been attributed to the constraints imposed by the lack of easily activated
13 slip systems, rather than its SFE [16]. In fact the primary grain refinement in magnesium alloys
14 during SPD methods is characterized by the nucleation of fine grains along the prior GBs. This
15 is attributed to the development of stress concentrations at the boundaries and the subsequent
16 activation of both basal and non-basal slip processes [17].
17

18
19 The detailed study of the material deformed in the early stages of the ABE process
20 reveals that the majority of DRXed grains formed during the first ABE pass are originated from
21 grain boundary bulging micro-mechanism, often called strain-induced boundary migration
22 (Fig. 3a). The formation of new grains by the latter mechanism was also confirmed through
23 local misorientation measurements by EBSD (Fig. 3b). It is believed that the local boundary
24 migration occurs where there is a stored energy difference across a high-angle boundary.
25 Accordingly, the migrating boundary is anchored by the pre-existing cell/subGBs and a grain
26 boundary bulge develops [17]. However, in the case of AZ31 magnesium alloy, cells/subgrains
27 have been hardly found. Instead, it has been demonstrated that after bulging out a segment of
28 grain boundary, a bridging dislocation wall forms between the bulged region and the parent
29 grain. During further deformation, the misorientation of this bridging wall gradually increases,
30 and the bulged region becomes a DRXed grain [18].
31

32
33 FE-SEM was performed to obtain detailed information about the microstructure evolution
34 developed after the second ABE pass. The FE-SEM micrograph in Fig. 4 clearly shows that ultra
35 fine grains (around 1 μm) have been formed in the recrystallized area during the second ABE
36 pass. The latter observation points out that additional refinement is achieved through applying
37 the second pass.
38

39
40 The earlier studies on DRX in AZ31 alloy have denoted that the recrystallized grains
41 remain virtually unchanged as deformation proceeds [19]. It has also been observed during
42 ECAP of AZ31 alloy that once dynamic recrystallization takes place and new grains are formed,
43
44
45

dislocation density will decrease sharply at these regions. In successive pass, the generated dislocations through further deformation will accumulate in the initial coarse grains and consequently induce dynamic recrystallization at these places. Therefore, the fraction of fine grains increases with ECAP pass number [20, 21]. This ends to the substitution of initial grains by DRX fine grains during subsequent deformation pass, but no evolution was considered for the pre-formed DRX grains. In addition Ding et al. believed [19] that the size of the fine grains obtained during ECAP was not gradually refined by successive extrusion passes. However, in the present work the additional refinement of the pre-formed DRXed grains has been achieved upon subsequent straining during the second pass.

To understand the detailed mechanism of fine grains evolution and their further refinement during successive ABE passes, EBSD maps of the material deformed to middle stage of second and third ABE passes are depicted in Fig. 5. It is worth noting that new boundaries with low to medium angle misorientation are developed within the grains. These low angle boundaries (LABs) are mainly characterized by 5 to 15° misorientation (the green and red lines in the map) and transverse the grain interior. It appears that, upon further straining, the LABs transform into high angle boundaries (HABs) and subdivide the DRXed grains to finer ones. This is typically considered as continuous grain refinement.

In order to precisely characterize this repetitive grain refinement, the boundary spacing histogram was measured for the experimental material deformed to different passes, through counting the HABs and LABs characterized by $>5^\circ$ misorientation. Thus, the histogram includes the distances between boundaries and sub-boundaries. As illustrated in Fig. 6, the boundary spacing curve shifts to smaller one with increasing strain, which denotes the development of new LAB and HABs within prior grains. This evolution brings the smallest average spacing down to about 0.5 μm after four passes. Earlier studies [22, 23] have separated such boundaries into two groups: (i) geometrically necessary boundaries separating crystallites that deform by different selections of slip systems and/or different strain or strain amplitudes and (ii) incidental dislocation boundaries formed by the trapping of glide dislocations. These boundaries can originate from GBs as well as dislocation arrays in the deformed metals, and subdivide the grain into regions that are smaller than the original grain size. The latter trend is called repetitive refinement, where a given recrystallized grain is subdivided (recrystallized) repeatedly to finer

ones during consequence of deformation passes. Previous reports have not traced no evolution for the and it is the first-time observation in magnesium alloy during SPD processing.

It is suggested that the crystallographic slip operates more homogeneous and bulging mechanism ceases during subsequent passes because of the achieved fine grain sizes during prior deformation pass. Twinning is also suppressed at smaller grain size [24]. This means a decrease in contribution of twin DRX mechanism to the overall deformation behavior in finer grain sizes. However, the presence of LABs during the second and third passes is well representative of the high efficiency of dynamic recovery. This suggests that a higher portion of non-basal slip can be activated in fine grained Mg alloys [25]; which gives rise to the higher share of dynamic recovery and the development of LABs. These features should be promoted by the deformation temperatures involved. Trapping of dislocation by LABs during subsequent deformation would result in gradual increase in their misorientation and transforming to high angle ones, i.e. CDRX. Therefore, dislocation slip and potent recovery are responsible for the occurrence of CDRX in the mantle region of the grains. This is confirmed by the surface observations made by Sitdikov and Kaibyshev [26] in hot deformed pure magnesium [27], where the occurrence of multiple slip near prior GBs may result in two dimensional nucleus [26] that play an important role in the operation of CDRX [16, 28]. The results are also consistent with the conclusion that the rearrangement of lattice dislocation belonging to different slip systems of either basal or non-basal can result in the formation of LABs [25]. Thus, CDRX mechanism, which typically observes in materials with high SFE, occurs in the fine-grained magnesium during the latter ABE passes. This means that a change in the DRX mechanisms (from DDRX toward CDRX) may take place as the deformation passes is increased.

Figure 7 shows the distributions of the misorientation angles in terms of cumulative frequency (frequency of and below a given misorientation angle) of LABs and HABs in the samples ABEed at 330°C. It indicates that the frequency of LABs with misorientation angles below 15° increased after single ABE, which confirms the operation of extensive dynamic recovery. However, the frequency of LABs decreases but that of HABs increases with applying successive passes. The decrease in LABs (misorientation below 15°) may indicate the transformation of LABs to HABs by incorporating the dislocations that generate during deformation. The latter requires new grain boundary area to be continuously created during deformation [29]. This is consistent with the increase in frequency of HABs.

As it is well established the CDRX is essentially a one-step phenomena, i.e. new grains are formed homogenously throughout the material and can hardly grow [25, 29]. In contrast, the nucleation of new grains by DDRX is followed by their long distance migration [14]. Thus, finer grain sizes may be expected during CDRX. Accordingly the operation of CDRX in fine grains (formed through DDRX during earlier passes) may result in further refinement during successive passes. This is in agreement with the present results on evolution of mean grain sizes and fraction of recrystallized area in Fig. 8, which was measured over the whole map area including new and old grains. It is interesting to note that in Fig. 8 as the successive passes increases, the mean grain size is significantly reduced, even though the fraction of dynamically developed grains hardly increase or remains constant. The decrease in mean crystallite size is then slowing down until a steady state value (2 μm) is reached. This is the case that was attained after four ABE passes and therefore further straining through fifth and sixth passes was not associated with further grain refinement. It should be noted that as the grains continue to refine by successive passes the formation of LABs is suppressed (see Fig. 8). This is related to the fact that the HABs can efficiently absorb the dynamically generated dislocations [31]. The simulation of microstructural evolution during CDRX has denoted that at such large strains the dynamic recovery alone is unable to justify the restoration of microstructure [32] and that misorientations are mainly increased by grain boundary sliding [33]. The latter analogy may be held for SPD of magnesium alloys to very large strain at such a high temperatures (330 °C).

4. Conclusion

In summary, discontinuous dynamic recrystallization was found as the dominant grain refinement mechanism in AZ31 experimental alloy during the early ABE pass, thereafter the dynamically recrystallized grains, in turn, were repetitively refined through continuous dynamic recrystallization upon applying successive passes. This was associated with the formation of low angle boundaries and gradual transformation to high angle boundaries. The decrease in grain size was reached to a steady state of about 2 μm by applying four passes, after that efficient absorption of dislocation by high angle boundaries and possibly grain boundary sliding may explain the microstructural evolutions.

References

- [1] W. Kim, H. Jeong, H. Jeong, Scripta Materialia. 61 (2009) 1040.
- [2] Y.T. Zhu, T.C. Lowe, T.G. Langdon, Scripta Materialia. 51 (2004) 825.
- [3] D. Orlov, G. Raab, T.T. Lamark, M. Popov, Y. Estrin, Acta Materialia. 59 (2011) 375.
- [4] J. Del Valle, F. Carreno, O. Ruano, Acta Materialia. 54 (2006) 4247.
- [5] Q. Yang and A.K. Ghosh, "Deformation behavior of ultrafine-grain (UFG) AZ31B Mg alloy at room temperature", Acta materialia, 2006, Vol. 54, 5159-5170.
- [6] R.B. Figueiredo, T.G. Langdon, Journal of materials science. (2010) 1.
- [7] C. Su, L. Lu, M. Lai, Materials Science and Engineering: A. 434 (2006) 227.
- [8] M. Perez-Prado, Scripta materialia. 51 (2004) 1093.
- [9] J. del Valle, F. Peñalba, O. Ruano, Materials Science and Engineering: A. 467 (2007) 165.
- [10] S. Fatemi-Varzaneh, A. Zarei-Hanzaki, Materials Science and Engineering: A. 504 (2009) 104.
- [11] S. Fatemi-Varzaneh, A. Zarei-Hanzaki, Materials Science and Engineering: A. (2010).
- [12] S. Fatemi-Varzaneh, A. Zarei-Hanzaki, S. Izadi, Journal of materials science. (2011) 1.
- [13] S. Gourdet, F. Montheillet, Acta Materialia, 51 (2003) 2685.
- [14] S. Fatemi-Varzaneh, A. Zarei-Hanzaki, H. Beladi, Materials Science and Engineering: A. 456 (2007) 52.
- [15] C. Chang, X. Du, J. Huang, Scripta Materialia. 59 (2008) 356.
- [16] R. Kaibyshev, O. Sitdikov, Physics of metals and metallography. 73 (1992) 635.
- [17] A. Galiyev, R. Kaibyshev, G. Gottstein, Acta Materialia. 49 (2001) 1199.
- [18] D. Sun, C. Chang, P. Kao, Metallurgical and Materials Transactions A. 41 (2010) 1864.
- [19] S. Ding, C. Chang, P. Kao, Metallurgical and Materials Transactions A. 40 (2009) 415.
- [20] L. Yuanyuan, Z. Datong, C. Weiping, L. Ying, G. Guowen, Journal of Materials Science. 39 (2004) 3759.
- [21] W. Kim, C. An, Y. Kim, S. Hong, Scripta Materialia. 47 (2002) 39.
- [22] Q. Liu, D. Juul Jensen, N. Hansen, Acta Materialia. 46 (1998) 5819.
- [23] D. Hughes, N. Hansen, Acta materialia. 45 (1997) 3871.
- [24] P. Dobron, F. Chmelík, S. Yi, K. Parfenenko, D. Letzig, J. Bohlen, Scripta Materialia. 65 (2011) 424.
- [24] J. Koike, New deformation mechanisms in fine-grain Mg alloys, in, Trans Tech Publ, 2003, pp. 189.
- [26] O. Sitdikov, R. Kaibyshev, Materials transactions-JIM. 42 (2001) 1928.
- [27] R. kaibyshev, O. Sitdikov, on bulging mechanism of dynamic recrystallisation in: Third International Conference on Recrystallization and Related Phenomena, 1996, 312.
- [28] M. Perez-Prado, J. Del Valle, J. Contreras, O. Ruano, Scripta Materialia. 50 (2004) 661.
- [29] J.W. Cahn, Y. Mishin, A. Suzuki, Acta Materialia. 54 (2006) 4953.
- [30] H. McQueen, M. Kassner, Scripta materialia. 51 (2004) 461.
- [31] R. Kaibyshev, A. Galiev, O. Sitdikov, Nanostructured Materials. 6 (1995) 621.
- [32] S. Gourdet, F. Montheillet, Acta Materialia. 51 (2003) 2685.
- [33] R. Kaibyshev, A. Goloborodko, F. Musin, I. Nikulin, T. Sakai, Mat. trans. 43 (2002) 2408.

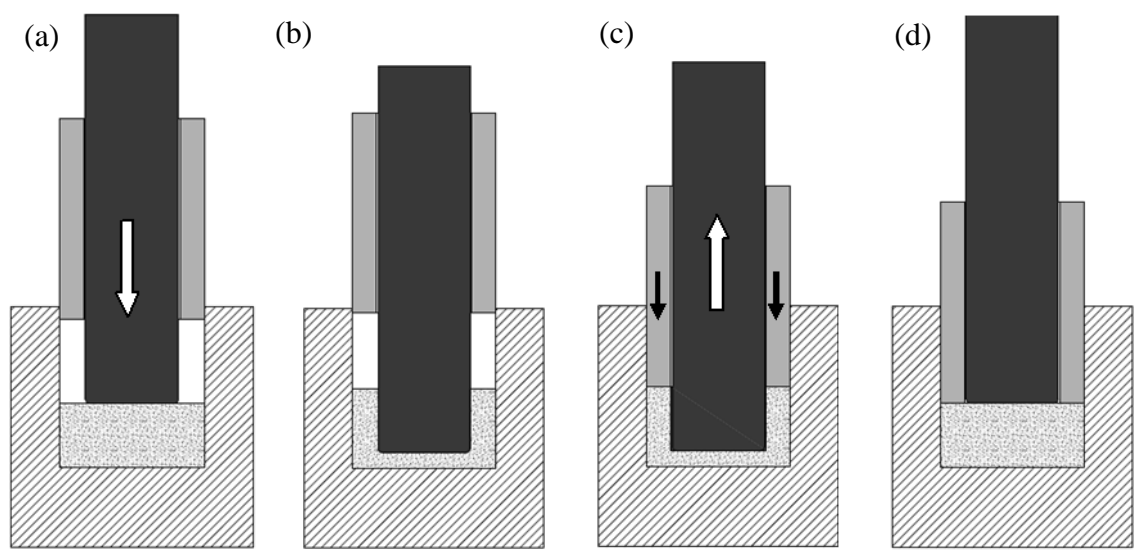


Fig. 1. The schematic illustration of ABE processing: (a) initial state, (b) step one, back extrusion, (c) step two, compression back and (d) end of process [10].

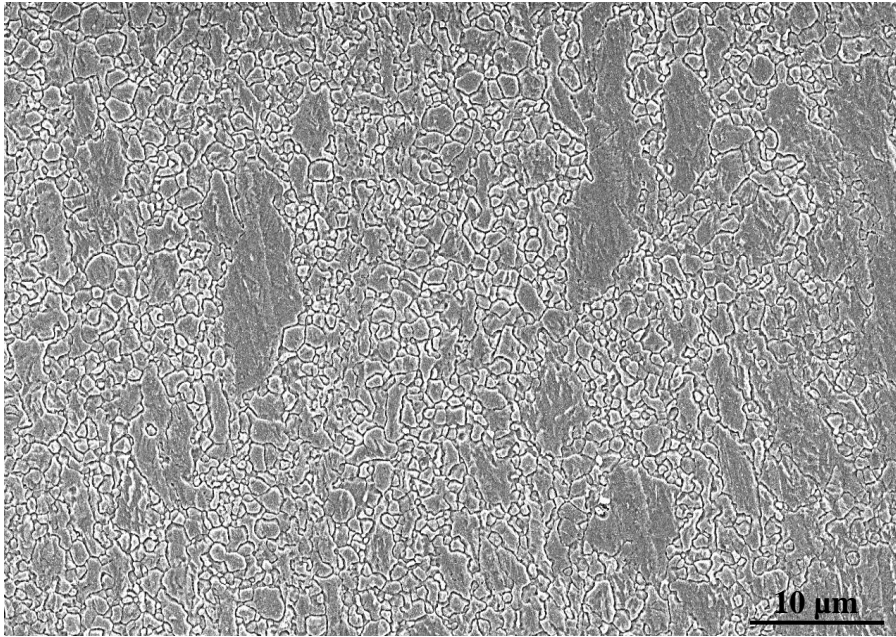


Fig. 2. The FE-SEM micrograph of AZ31 alloy after single ABE pass.

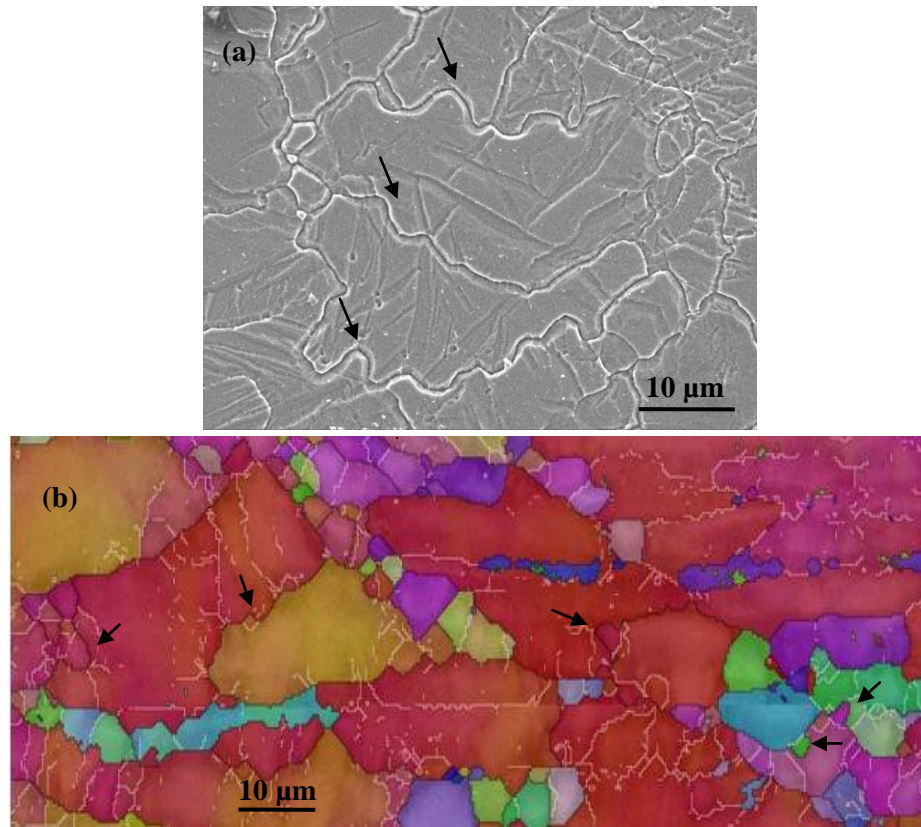


Fig. 3 a) and b) The microstructure of AZ31 alloy deformed to the first step of ABE process showing the bulging of GBs.

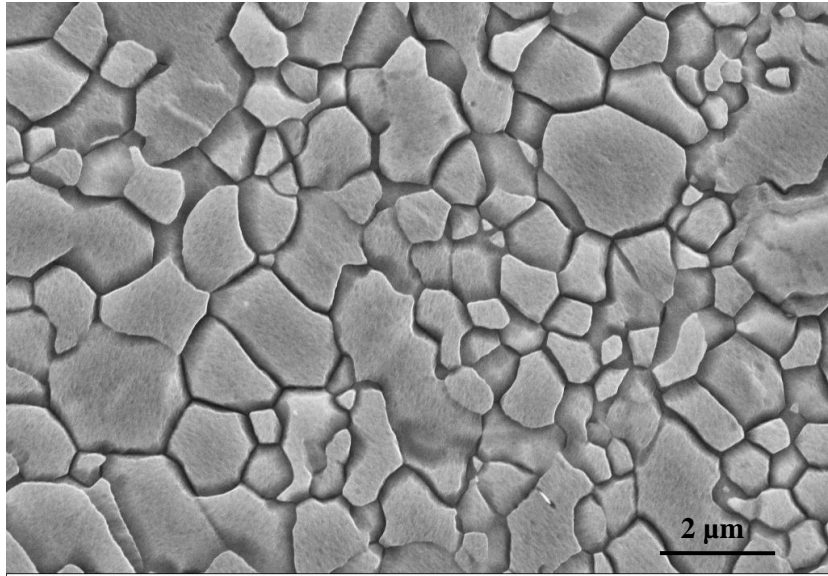


Fig. 4. The FE-SEM micrograph of AZ31 alloy after two ABE passes.

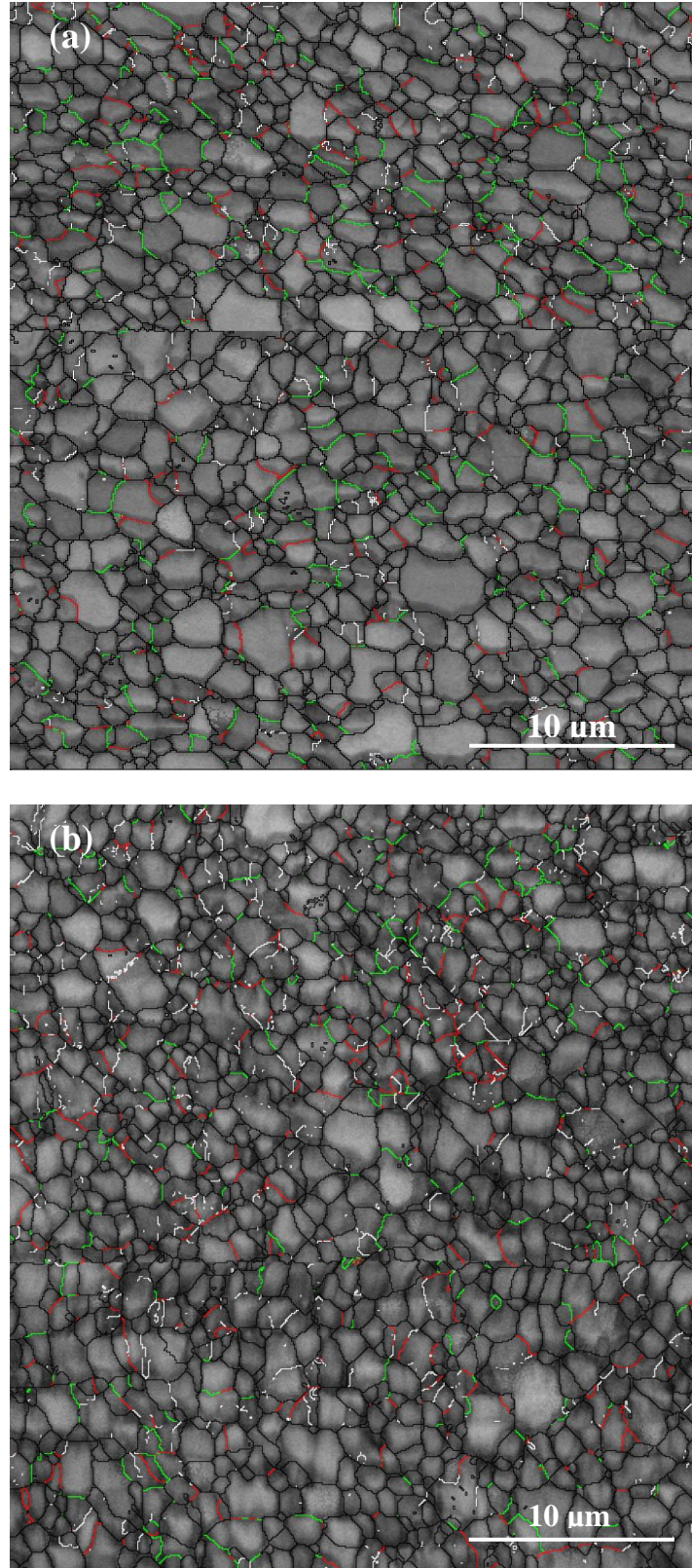


Fig. 5. The EBSD map of AZ31 alloy deformed to a) the second ABE pass, b) the third ABE pass (white lines: 2-5°, red lines: 5-10°, green lines: 10-15°, black lines: above 15° misorientation).

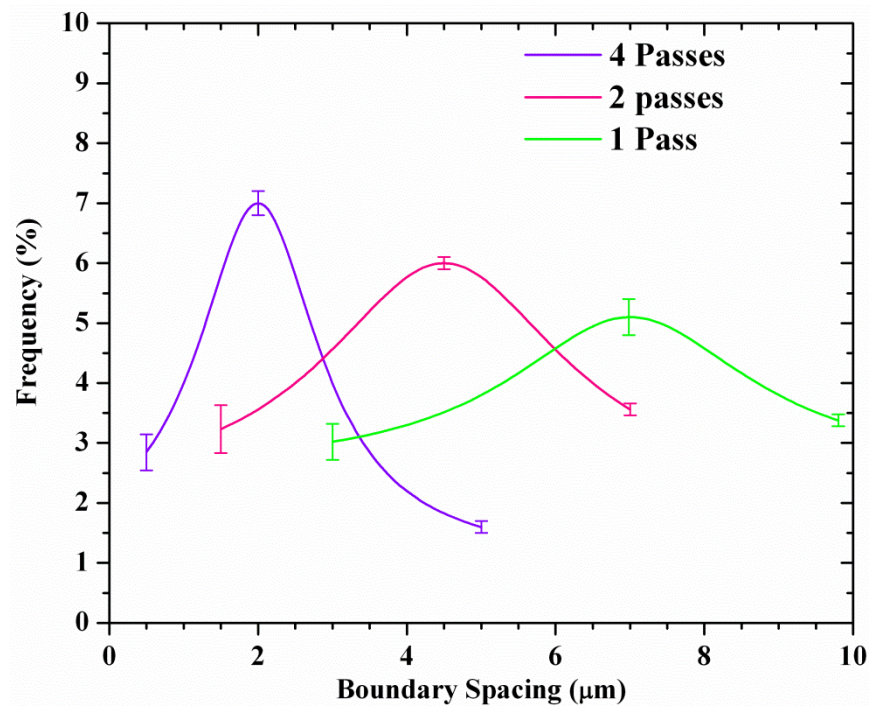


Fig.6. Boundary spacing histogram in AZ31 alloy deformed to various number of ABE passes.

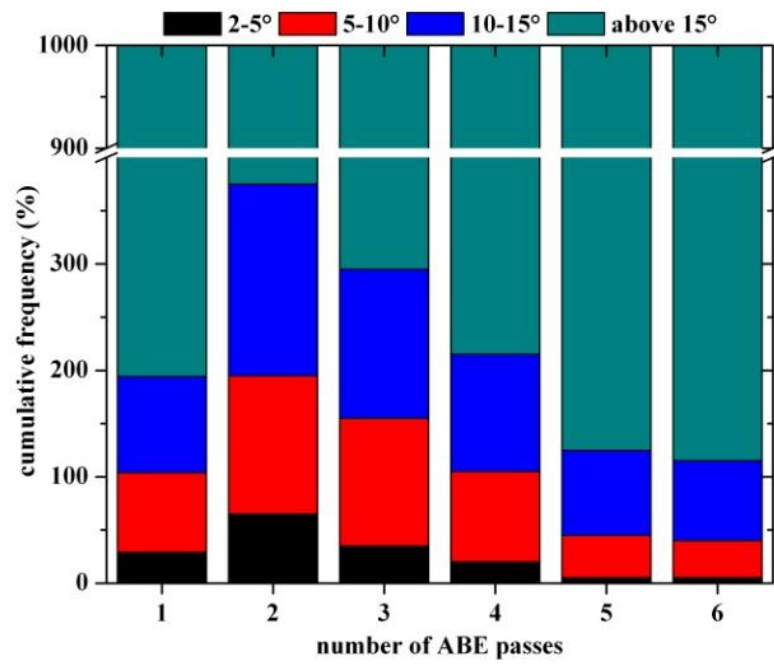


Fig. 7. The cumulative frequency of boundaries with different misorientation angle in AZ31 alloy deformed to various number of ABE passes.

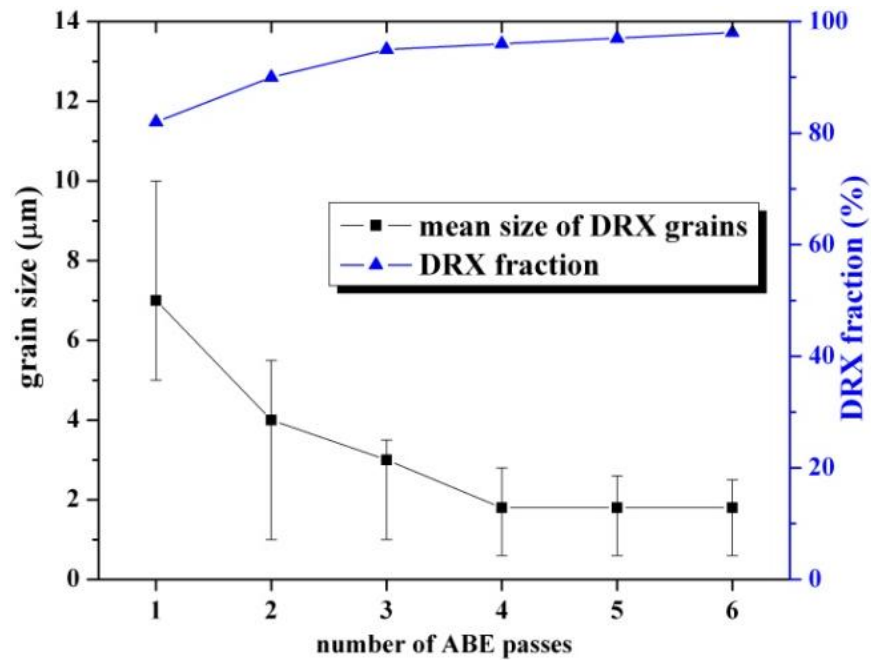


Fig. 8. The variation of mean grain size and DRX fraction with the number of ABE passes